# Several Considerations Regarding the Variable Blade Length Rotor

Bogdan Popescu* and Victor Giurgiutiu†
*Institute for Theoretical and Experimental Analysis of Aeronautical Structures, STRAERO S.A., R-77538 Bucharest, Romania*

## Introduction

SINCE the revolutionary breakthrough of Cierva and the engineering achievements of Sikorsky, the general layout of the conventional helicopter rotor has not changed much.[1] Though popular and widespread, this arrangement has some major limitations, one of the principal ones being the unsymmetric loading of the rotor disc. Serious difficulties also appear at the tip of the advancing blade (Mach number effects), and at the inner region of the retreating blade (reverse flow). Hence, significant research is still carried out to properly model the blade oscillatory aerodynamics in forward flight, with nonlinear unsteady effects being currently considered using advanced computational techniques.[2,3]

However, the reader's attention is drawn to the fact that there are alternative designs for dealing with some of these problems. One of these alternative designs is the advancing blade concept (ABC) in which two counter-rotating coaxial rotors are used, thus somehow balancing the global loading. However, the ABC design is still not free from Mach number effects on the advancing tip, and needs to deal with the additional constraint of preventing the counter-rotating blades contacting each other while flapping.

Another alternative design is the variable length blade (VLB). The increase in tip Mach number on the advancing blade is compensated by the reduction in blade length, with a complementary effect taking place on the retreating blade (cyclic VLB). Or one can decrease the overall rotor diameter as flight speed increases (collective VLB). Such concepts were studied in some depth about two decades ago,[4-6] and their merits and limitations were highlighted. But, due to technological difficulties at that time, the VLB concept did not pass the research stage. However, with the recent years developments in active control and smart materials technologies, it is the belief of the authors that this alternative design should be given a fresh re-evaluation.

## Variable Length Blade Concept

Figure 1 presents a variable radius rotor of a four-blade configuration. Elastic elements $k$ are used to create a simple harmonic oscillator tuned to the blade angular speed, thus allowing the blade pair to move in and out with ease under near resonance conditions. The active control of the blade movement can be achieved through a convenient smart materials application, as, e.g., a linear piezoelectric actuator.[7]

Considering a harmonic radial motion of the blade, we write the distance from the shaft to the inner end of the blade as

$$x_e(t) = x_{e0}[1 + h\cos(\Omega t - \varphi)] \tag{1}$$

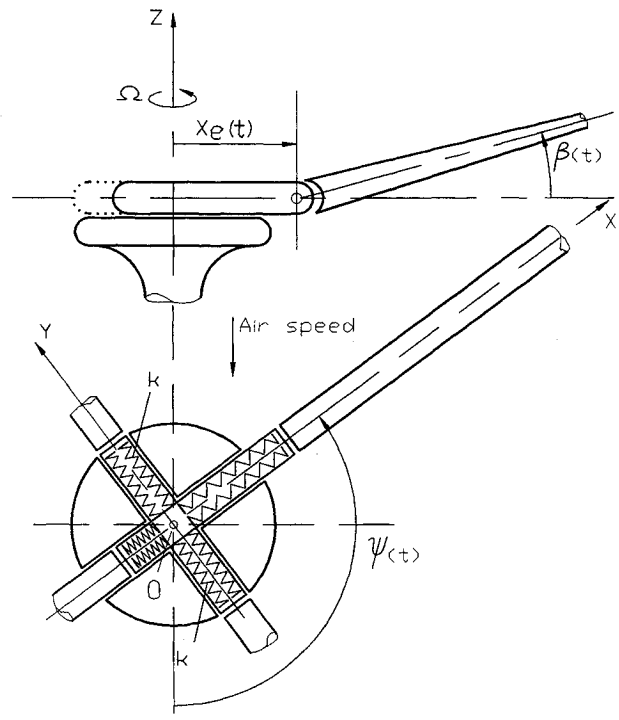


**Fig. 1 Possible VLB design.**

where $x_{e0}$ is the static position of the blade inner end, $\Omega$ the angular velocity of the rotor, $\varphi$ a phase angle, and $h = x_a/x_{e0}$ the VBL ratio, with $x_a$ being the oscillation amplitude. The distances were made dimensionless using the blade length $R$.

Two pairs of springs (Fig. 1) are provided for compensating the inertial and centrifugal forces and for creating the elastic restoring forces during the blade radial oscillation. Thus

$$M_s\ddot{x}_e + c\dot{x}_e + (4k - M_s\Omega^2)(x_e - x_{e0}) = F_{ex} \tag{2}$$

where $k = M_s\Omega^2/2$ is the stiffness of one spring, $M_s$ the mass of the blade pair, $c$ the damping coefficient, and $F_{ex}$ the axial excitation force.

The following assumptions are considered:

1) The spanwise flow on the blade has a negligible effect upon the flapping aerodynamics.

2) The total pitch angle referred to the shaft plane is in phase with the radial movement and given by

$$\theta(t) = \theta_0 + \theta_a\cos(\Omega t - \varphi) \tag{3}$$

3) The rotor shaft is fixed as in a wind-tunnel experiment. This simplifies the procedure and does not affect the conclusions in a broad sense. Hence, the shaft plane is fixed with respect to the air velocity direction.

The rotor equilibrium was studied using the basic equations of rigid body dynamics as applied to a blade pair. A relative motion composed of a rotation and a translation was considered. The shaft reaction forces and moments due to the motion of a blade pair were obtained applying the linear and angular momentum theorems. Then, through the change of variables, $\varphi' = \varphi + \pi/2$, the reaction forces and moments for the orthogonal blade pair were obtained. The reaction forces of the two blade pairs add up to zero, such that the inertia and Coriolis forces created by the axial movement of one blade pair are balanced by those due to the other blade pair. On the other hand, the blade is subject to an additional variable centrifugal force

$$F^*_{cf}(t) = -M_s\Omega^2(x_aR)\cos(\Omega t - \varphi) \tag{4}$$

which should be considered in fatigue evaluations.

Received July 13, 1992; revision received April 28, 1993; accepted for publication May 8, 1993. 

*Research Scientist; currently Visiting Research Scientist at ICA, University of Stuttgart, Pfaffenwaldring 27, 7000 Stuttgart 80, Germany.

†President-Director General; currently Visiting Professor at Virginia Polytechnic Institute and State University, Engineering Science and Mechanics Department, VA 24061. Senior Member AIAA.

The dynamic response of the blade flapping motion was calculated using Bramwell's procedure based on Euler's equations.[8] Considering a reference system fixed in the blade, and referring the flapping angle $\beta(t)$ to the shaft plane, one gets the flapping equation:

$$\ddot{\beta} + \Omega^2\{1 + \varepsilon[1 + 2h\cos(\Omega t - \varphi)]\}\beta = M_A/J_y \quad (5)$$

where $M_A$ is the aerodynamic moment, and $\varepsilon = x_{e0}x_g mR^2/J_y$ an eccentricity parameter, with $m$ the blade mass, $x_g$ its c.g. position, and $J_y$ the mass moment of inertia about the $y$ axis. The $h$ parameter controls the additional effects due to blade axial movement. For $h = 0$, one recovers the conventional case with the blade performing no axial oscillations. For $h > 0$, one gets increasing VLB effects. Practical values of $g$ are restricted to $g < 0.9$.

The flapping motion was assumed harmonical[8]

$$\beta(t) = a_0 - a_1\cos\Omega t - b_1\sin\Omega t \quad (6)$$

and the aerodynamic moment was taken in the form[9]

$$M_A(t) = \gamma(K_1\dot{\beta} + K_2\beta + K_3) \quad (7)$$

where $\gamma$ is Lock's number, and $K_1$, $K_2$, $K_3$ are expressions of $t$ and $x_e(t)$. The aerodynamic moment (7) was substituted into (5), and the resulting second-order ordinary differential equation (ODE) was set up as a system of first-order

$$\{\dot{q}\} = [A]\{q\} + \{B\} \quad (8)$$

where $\{q\}^T = [\dot{\beta}, \beta]$, while $[A]$ and $\{B\}$ are time-dependent coefficient matrices.

## Numerical Results

As a numerical illustration we considered a medium-size helicopter rotor at high forward speed. Common values for the lift slope $a$, blade chord $c$, and advance ratio $\mu$ were used. The flap response of the blade (Fig. 2) was calculated using an integrating procedure based on the Floquet theory and Runge-Kutta quadrature.[10] Two values of the axial motion parameter $h$ were used. In the first case the value $h = 0$ was modeling a conventional blade system. In the second case the value $h = 0.9$ was used to signify our proposed design. Comparative plots are presented in Fig. 2.

Several values of cyclic pitch $\theta_a$ and phase angle $\varphi$ combinations were employed. For $\theta_a = 13$ deg and $\varphi = -90$ deg, the largest improvement was obtained in reducing the maximum value of the flapping angle $\beta(t)$. For $\theta_a = 15$ deg and $\varphi = -90$ deg, the largest decrease was obtained in the minimum value of $\beta(t)$. However, the combination $\theta_a = 13$ deg, $\varphi = -65$ deg gave a flat response of the flapping angle over more than half of the circumferential travel. For $h = 0.9$ this was improved even further (Fig. 2).

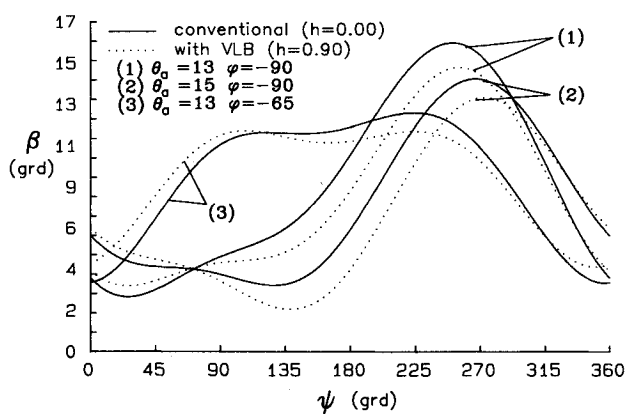


**Fig. 2 Blade flap response with and without VLB effects ($\mu = 0.4$, $m = 70$ kg, $R = 7$ m, $\Omega = 27$ rad/s, $x_{e0} = 0.05$, $x_g = 0.4$, $a = 5.7$, $c = 0.4$ m).**

## Discussion

The merits of the VLB concept stem from several directions. First, one should consider the increase in forward speed that can be achieved through the reduction of Mach number effects. For $h = 0$, the local airspeed at the conventional blade tip is $V + \Omega R$. For $h = 0.9$, the local airspeed at the VLB tip is $V + \Omega R(1 - hx_{e0})$. For typical values $x_{e0} = 0.05$ and $\Omega R = 169$ m/s, one gets a maximum increase of $\Omega R x_{e0} = 8.5$ m/s at $h = 0.9$. This means more than 10% increase in the helicopter forward speed of, e.g., $V = 75$ m/s, as considered in our example.

Secondly, one gets the benefit of reduced flapping motion as illustrated in Fig. 2. (A typical reduction of 10% can be quoted.) The reduction in flapping response has several beneficial repercussions upon the aerodynamic and structural behavior of the helicopter, among them the decrease of the unsteady aerodynamic forces, and therefore, the decrease of the fuselage vibration levels. Improvement in fatigue behavior should also be mentioned.

Another effect highlighted by our study regards the amount of cyclic pitch needed to achieve a certain blade flapping response. It can be seen in Fig. 2 that the addition of VLB effect ($h = 0.9$) shifts the apparent operating point from the $\theta_a = 13$-deg curve to the intermediate $\theta_a = 14$-deg curve. This means a 7% reduction in cyclic pitch, thus taking the operating point further away from the stall boundary.

The phase angle $\varphi$ involved in the cyclic motion was found to play a significant role in smoothing the flapping response. However, further studies of this effect will have to be undertaken with the inclusion of the lateral trim conditions. And although our study was based on a hinged flapping blade, the use of a hingeless design would provide a even better application of the VLB concept.

A possible weakness of the VLB concept may be found in the oscillatory axial force due to the radial motion of the blade. Equation (8) shows that this effect is at most in the ratio $x_{e0}/x_g$, i.e., about 10% of the steady axial load. Similarly, some oscillatory Coriolis forces appear in the transversal direction. Their fatigue consequences, though not negligible, are mild enough to be easily accommodated in the engineering design of the hub.

Another weakness of the VLB may be found in the controllability of blade axial motion. Very little was presented in this Note about the engineering details of this aspect, since various concepts connected with the actuation and control of blade axial movement are still under development. And a complete dynamic analysis (including body trim in both directions), ground- and air-resonance evaluations, and wind-tunnel tests on a model VLB rotor, will be considered in future research.

## References

[1]Young, W. R., *The Helicopters*, Time-Life Books, Alexandria, VA, 1982.

[2]Friedmann, P. P., "Helicopter Rotor Dynamics and Aeroelasticity: Some Key Ideas and Insights," *Vertica*, Vol. 14, No. 1, 1990, pp. 101–121.

[3]Johnson, W., "Airloads and Wake Models for a Comprehensive Helicopter Analysis," *Vertica*, Vol. 14, No. 3, 1990, pp. 255–300.

[4]Payne, P. R., *Helicopter Dynamics and Aerodynamics*, Pitman, London, 1959.

[5]Carter, E. S., "Impact of New Structural Concepts on System Capabilities," *Advanced Rotorcraft*, NASA, Langley Field, VA, NATO AGARD CP 121, 1973, pp. 13.1–13.11.

[6]Segel, R. M., and Fradenburgh, E. A., "Development of the TRAC Variable Diameter Rotor Concept," AIAA Paper 69-221; see also AIAA/AHS VTOL Research, Design, and Operations Meeting, Georgia Inst. of Technology, Atlanta, GA, Feb. 1969.

[7]Rogers, C. A., "Dynamic and Structural Control Utilizing Smart Materials and Structures," *Proceedings of the International Workshop on Intelligent Materials*, Tsukuba, Japan, 1989, pp. 109–121.

[8]Bramwell, A. R. S., *Helicopter Dynamics*, Arnold, London, 1976, pp. 154, 155.

[9]Popescu, B., and Giurgiutiu, V., "The Calculation and Design of the Oscillating Rotor," (in Romanian), STRAERO S.A., TR N-6076, Bucharest, Romania, June 1991.

[10]Friedmann, P. P., Hammond, C. E., and Tze-Hsin, W., "Efficient Numerical Treatment of Periodic Systems with Application to Stability Problems," *International Journal for Numerical Methods in Engineering*, Vol. 11, No. 7, 1977, pp. 1118–1122.

# Turbulence Model Evaluation for Use with Supercritical Airfoils

W. Kelly Londenberg*
*ViGYAN, Inc.,*
*Hampton, Virginia 23666*

## Nomenclature

$C_p$ = pressure coefficient
$c$ = chord
$c_l$ = sectional lift coefficient
$M$ = corrected Mach number
$R_N$ = Reynolds number based on chord
$x/c$ = nondimensional chord station
$y^+$ = law of the wall coordinate
$\alpha$ = angle of attack, deg
$\delta_a$ = aileron deflection, deg

## Introduction

INCREASING the efficiency of aircraft configurations in general, and transport aircraft in particular, is a never-ending task. With progress being made in the optimization of the cruise configuration of transport aircraft, efforts are now being made to increase the performance at off-design conditions, such as when ailerons are deflected, high-lift configurations, and near the buffet boundary. Small decreases in drag coefficient at off-design conditions can make significant improvements in the overall performance of the vehicle. For example, a 1% increase in takeoff $L/D$ is equivalent to a 2800-lb increase in payload, or a 150-nm increase in range for a typical large, twin-engine transport.[1] Any analysis or wind-tunnel testing of these viscous dominated flowfields must be done at conditions where the boundary-layer thickness and state are simulated. Since Reynolds number effects on aerodynamic data is not a linear function, this must be made at full-scale Reynolds number conditions to correctly simulate the boundary-layer profiles.

With the continuing advancement of computing power and algorithm efficiency, it has become more practical to calculate flows around aerospace vehicles at full-scale Reynolds number conditions. The use of the computer allows for the identification of problem areas, and therefore, the streamlining of the wind-tunnel test program. At cruise conditions, the flow is nonseparated and can easily be computed using full potential or Euler methods coupled with boundary-layer techniques. However, at off-design conditions, the flow may become separated and these simpler methods cannot accurately predict the flowfield. At these conditions Navier-Stokes solvers are required to predict the often complicated viscous-inviscid interactions that are occurring. Even with the increases in computer power and algorithm efficiency of recent years, turbulence quantities cannot yet be calculated directly, requiring the use of modeling techniques.

This Note will describe the evaluation of turbulence models as used for the analysis of a transport airfoil with deflected aileron at high Reynolds numbers and transonic Mach numbers. The turbulence models evaluated are the Baldwin-Lomax algebraic model,[2] the Johnson-King half-equation model,[3] and the Baldwin-Barth[4] and Spalart-Allmaras[5] one-equation models. The analysis code used is the NASA Langley thin layer Navier-Stokes solver CFL3D.[6]

## Results and Discussion

Solutions were calculated for the McDonnell Douglas Aerospace—Transport Aircraft Unit's DLBA032 12.3% chord thick supercritical airfoil. Experimental data were obtained for this airfoil at the Institute for Aerospace Research (IAR) 15- × 60-in. transonic wind tunnel. Force and pressure data were obtained for a wide range of angles of attack at Mach numbers corrected for both floor and ceiling wall effects, as well as for sidewall boundary effects using Murthy's methodology[7] of 0.716 at Reynolds number based on chord of 5, 15, and 25 million, and at $M = 0.747$ for $R_N = 15 \times 10^6$. Data was also obtained for aileron deflections ranging from −5 deg [trailing-edge up (TEU)] to +5 deg [trailing-edge down (TED)].

Based on a grid resolution study performed for this airfoil with nondeflected aileron at $\alpha = 1.2$ deg, $R_N = 15 \times 10^6$, and $M = 0.716$, it was determined that a C-grid with a mesh size of 289 × 65 (wraparound $x$ radial) with an outer boundary extent of $20c$ yielded results of acceptable accuracy.[8] Minimum spacing normal to the surface was $1.5 \times 10^{-6}c$, which resulted in $y^+$ values at one grid point off of the surface of near 1.

The computational grid at the trailing edge of the airfoil was found to have significant effects in the computed solutions. Varying the streamwise clustering at the trailing edge by 0.1% chord moved the location of the computed shock wave nearly 1% chord.[8] The sensitivity of the supercritical airfoil flowfield to trailing-edge clustering observed in this study is also evident in a study by Yu et al.[9] The streamwise clustering at the trailing edge of the airfoil selected for use in the present study was $0.1\%c$. The flowfield around the DLBA032 airfoil is also very sensitive to how the trailing edge is closed. Several methods of closing this blunt trailing edge (approximately $0.5\%c$ thick at the trailing edge) were tried. The only method that worked with all the turbulence models was that of averaging the upper and lower surface trailing-edge points.

Solutions were obtained for the DLBA032 airfoil using the Baldwin-Lomax, Johnson-King, Baldwin-Barth, and Spalart-Allmaras turbulence models. The same mesh was used for all Reynolds numbers. The resulting maximum $y^+$ values ranged from near 0.5 for $R_N = 5 \times 10^6$ to slightly greater than 1 for $R_N = 25 \times 10^6$. Transition was fixed for the calculations at the experimental transition grit location: $15\%c$ upper surface and $28\%c$ lower surface for $R_N = 5 \times 10^6$, $10\%c$ upper surface and $15\%c$ lower surface for $R_N = 15 \times 10^6$, and free transition (leading edge in the computations) for $R_N = 25 \times 10^6$.

The general effect of turbulence model on computed pressure distribution is shown in Fig. 1 for the airfoil with nondeflected aileron, and in Fig. 2 for the airfoil with 2-deg aileron deflection. These solutions were obtained for $M = 0.716$, and $\alpha = 1.20$ deg for $\delta_a = 0$ deg, and $\alpha = 1.24$ deg for $\delta_a = 2$ deg. All models predict pressures that are generally in good agreement with experimental pressures for the nonde-

Presented as Paper 93-0191 at the AIAA 31st Aerospace Sciences Meeting and Exhibit, Reno, NV, Jan. 11–14, 1993; received March 1, 1993; revision received May 13, 1993; accepted for publication May 13, 1993. 

*Research Engineer, 30 Research Drive. Member AIAA.